Expert diagnostic system for moving-coil loudspeakers using nonlinear modeling

Mingsian R. Bai[a] and Chau-Min Huang
Department of Mechanical Engineering, National Chiao-Tung University, 1001 Ta-Hsueh Road, Hsin-Chu 300, Taiwan

(Received 18 July 2008; revised 5 December 2008; accepted 8 December 2008)

This work aims at the development of an expert diagnostic system for moving-coil loudspeakers. Special emphasis is placed on the defects resulting from loudspeaker nonlinearities. As a loudspeaker operates in the large signal domain, nonlinear distortions may arise and impair sound quality. Analysis of nonlinear responses can shed light on potential design faults of a loudspeaker. By exploiting this fact, this expert diagnostic system enables classification of design faults using a defect database alongside an intelligent fault inference module. Six types of defects are investigated in this paper. A large signal model based on electromechanical analogous circuits is employed for generating the defect database, through which a neural-fuzzy network is utilized for inferring the defect types. Numerical simulations and experimental investigations were undertaken for validating the loudspeaker diagnostic system.
 [DOI: 10.1121/1.3058639]

PACS number(s): 43.38.Dv, 43.80.Qf [AJZ] Pages: 819–830

I. INTRODUCTION

As a loudspeaker operates in the large signal domain, nonlinear distortions may arise and can potentially impair sound quality. Nonlinear causes (Table I) may be attributed to faults resulting from the design or manufacturing process. Traditionally, diagnostics of loudspeakers rely on well trained human experts who are able to evaluate faulty loudspeakers according to the distortions or symptoms. However, human experts are scarce and require long training. Plus, human experts can make false judgments, especially after a long period of work. It is then highly desirable to analyze and diagnose loudspeakers in a systematic and efficient manner that is free of human errors. To address these issues, this paper aims to develop an expert diagnostic system for moving-coil loudspeakers with emphasis on nonlinear causes.

Nonlinear distortions of a loudspeaker may arise as a result of various causes such as nonlinear compliance, nonlinear force factor, nonlinear inductance, Doppler Effect, suspension creep, etc.,[1–3] as defined in an IEC standard PAS 62458. It is often insufficient to account for nonlinearities using linear loudspeaker models.[4] Since sound quality during audio reproduction may suffer due to nonlinear distortions, to be able to assess and classify nonlinear causes would be quite useful in the design phase and even in the manufacturing quality control phase of loudspeakers.[5–8] In the past, metrics including dc-displacement, harmonic distortion, intermodulation, etc., have been suggested to quantify loudspeaker nonlinearities.[9–12] On the other hand, large signal models[13–17] based on electrical equivalent circuits have been suggested for predicting the performance of a loudspeaker in the large signal domain. Remedies for nonlinear faults of loudspeaker have also been reported in literature.[18]

In this paper, we develop an expert system aimed at loudspeaker diagnostics by exploiting nonlinear signatures of loudspeaker responses. An expert system[18] comprises a computer program with feature extraction, knowledge, and inference procedure, which mimics a human expert in analyzing problems and making decisions. Expert system has found many applications in automatic diagnosis, prediction, and control since the advent of the artificial intelligence. The loudspeaker diagnostic system in this paper is developed in two major steps: (1) creation of a cause-symptom database via a nonlinear loudspeaker model based on electrical equivalent circuits, and (2) training the neural-fuzzy network using the database. The loudspeaker diagnostic process begins with measuring numerous nonlinear metrics (symptoms) using a distortion analyzer and then deduce the fault types (causes) automatically via the neural-fuzzy network.

In the proposed system, the expert diagnostic system seeks to infer potential defect types in lieu of human experts, by using a loudspeaker cause-symptom database. The inference engine is constructed on the basis of neural-fuzzy networks. Fuzzy logic[19] was first introduced by Zadeh in 1965. Fuzzy logic mimics human reasoning that allows for some "fuzzy" latitude in making decisions. Neural network[20,21] (NN) is another technology that enables realizing human intelligence in machines. Recently, neural-fuzzy systems [fuzzy neural network (FNN)] (Refs. 21 and 22) that exploit the combined advantages of fuzzy logic and NN have received increasing interest in the AI research. For example, a five-layered FNN (Ref. 22) suggested by Becraft and Isermann[23] is widely used in many problems. Lin's five-layered FNN is also employed in this paper to investigate nonlinear diagnostic problem of moving-coil loudspeakers.

The expert diagnostic system in this paper is implemented on a notebook computer, with the aid of a nonlinear

[a]Author to whom correspondence should be addressed. Electronic mail: msbai@mail.nctu.edu.tw

TABLE I. Nomenclature of nonlinear loudspeaker model.

State variables	Unit	Interpretation
$u(t)$	V	The driving voltage at loudspeaker terminals
$x(t)$	mm	Displacement of the voice coil
$v(t)$	mm/s	Velocity of the voice coil
$i(t)$	A	The electric input current
$i_2(t)$	A	The current through L_2
Electrical parameters	**Unit**	**Interpretation**
$R_E(T_V)$	Ω	dc resistance of voice coil
$L_E(x)$	mH	Part of the voice coil inductance
$L_2(x)$	mH	Parainductance of the voice coil
$R_2(x)$	Ω	Electric resistance caused by eddy currents
Mechanical parameters	**Unit**	**Interpretation**
$Bl(x)$	N/A	The force factor
$F_m(x,i,i_2)$	N	The reluctance force
$C_{\mathrm{MS}}(x)$	mm/N	Mechanical compliance of driver suspension [theinverse of stiffness $K_{\mathrm{MS}}(x)$]
R_{MS}	kg/s	Mechanical resistance of driver suspension losses
M_{MS}	kg	Mechanical mass of driver diaphragm assembly including voice- coil and air load
Thermal model	**Unit**	**Interpretation**
R_{TV}	K/W	Thermal resistance of path from coil to magnet
R_{TM}	K/W	Thermal resistance of magnet structure to ambient air
C_{TV}	J/K	Thermal capacitance of voice coil and nearby surroundings
C_{TM}	J/K	Thermal capacitance of magnet structure
$P(t)$	W	Real electric input power
$T_V(t)$	K	Temperature of the voice coil
$\Delta T_V(t)$	K	$\Delta T_V(t)=T_V(t)-T_A$, increase in voice coil temperature
$T_M(t)$	K	Temperature of the magnet structure
$\Delta T_M(t)$	K	$\Delta T_M(t)=T_M(t)-T_A$
T_A	K	Ambient temperature
δ	K^{-1}	$\delta=0.003\,93\ \mathrm{K}^{-1}$ for copper and $\delta=0.003\,93\ \mathrm{K}^{-1}$ foraluminum.

analyzer equipped with a laser vibrometer. Two sample loudspeakers were employed in the case studies to validate the expert system. The experimental results will be discussed and summarized in Sec. V.

II. THE LARGE-SIGNAL MODEL OF MOVING-COIL LOUDSPEAKERS

As an electroacoustic transducer, a moving-coil loudspeaker [Fig. 1(a)] involves energy conversion and coupling among the electrical, mechanical, and acoustical domains. At low frequencies where the wavelength is large in comparison to the geometric dimensions, the state of a loudspeaker can be described simply by a lumped parameter model that can be represented by a generic equivalent circuit in Fig. 1(b) Note that, in contrast to the small signal model, the force factor $Bl(x)$, mechanical compliance $C_{\mathrm{MS}}(x)$, and voice coil inductance $L_E(x)$ are not constant, but varying with the displacement of the voice coil.[8]

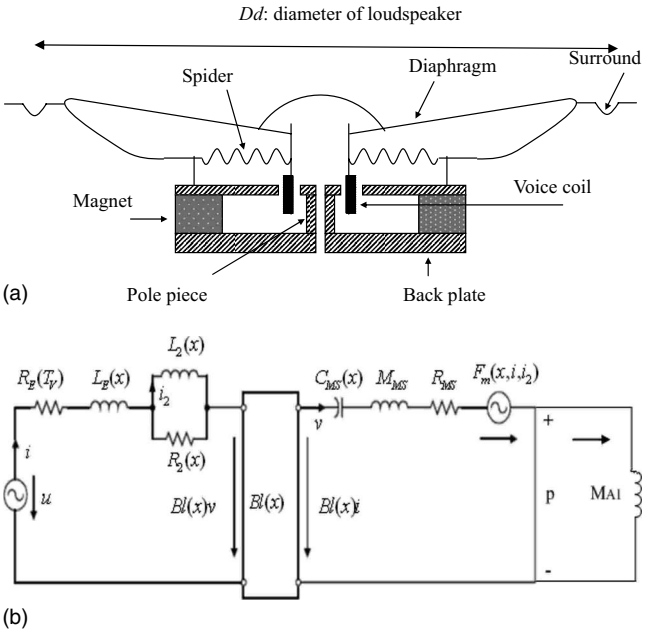

FIG. 1. Electroacoustic analogy of a moving-coil loudspeaker. (a) The physical structure. (b) The equivalent circuit.

A. Nonlinearities of moving-coil loudspeakers

1. Loudspeaker stiffness $K_{\mathrm{MS}}(x)$

Like a mechanical spring, a suspension system[9,10] is used to generate a restoring force for a loudspeaker, pulling the voice coil back to its rest position.[10,11]

2. Force factor $Bl(x)$

The force factor $Bl(x)$ (Ref. 9) serves as the coupling between the mechanical and electrical domains of a moving-coil loudspeaker, where B is flux density and l is the length of the voice coil in the magnet air gap. The force factor $Bl(x)$ may result in two nonlinear effects: (a) back electromotive force and (b) Lorentz force $F=Bl(x)i$.

3. Voice coil inductance $L_E(x)$

Inductance $L_E(x)$ (Refs. 9 and 12) that varies with displacement is another source of loudspeaker nonlinearity. The magnetic flux is dependent on the position of the coil and the magnitude of the current and frequency.[9,12]

4. Other nonlinearities

In addition to the preceding nonlinearities,[9,10] several other nonlinearities are included in this paper.

A. Doppler effect. Large cone excursions occur at low frequencies during loudspeaker operations. This mechanism may be described by the product of displacement and differentiated sound pressure and requires low and high frequency components at the same time. If the distance between the source and the listener can vary drastically to give rise to time delay modulation of sound pressure signals, the Doppler effect may lead to intermodulations in the high frequency regime.

B. Reluctance force F_m. The displacement-varying $L_E(x)$ may introduce an additional reluctance force

C. Parainductance and the resistance caused by eddy currents. Ideal linear inductance is not sufficient for modeling the phenomenon that electrical impedance increases at higher frequencies due to the inductance loss.

D. Rub and buzz (Refs. 25 and 26). This kind of distortion occurs when the voice coil rubs on the pole tips, the lead wire strikes the diaphragm, or a loose glue joint starts vibrating. This is especially a common cause of nonlinear distortion for small speakers or microspeakers, where overdriven operation tends to exceed the mechanical design limits such as the air gap and the excursion limit.

B. Large signal model

Traditional linear models[4] are insufficient for predicting large signal behavior of loudspeakers. Clearly, the large signal model[13–17] is a preferred way to simulate nonlinear effects such as nonlinear distortions and the dc-component of the cone displacement. The large signal model considers the loudspeaker as a coupled electrical-mechanical-acoustical system with nonlinear parameters, as shown in Fig. 1(b).

The dynamics of Fig. 1(b) can be described using the following differential equations:

$$u = iR_E(T_V) + \frac{d(L_E(x)i)}{dt} + \frac{d(L_2(x)i_2)}{dt} + Bl(x)v, \tag{1}$$

$$\frac{d(L_2(x)i_2)}{dt} = (i - i_2)R_2(x), \tag{2}$$

$$Bl(x)i - F_m(x,i,i_2) = (M_{\mathrm{MS}} + M_{A1})\frac{d^2x}{dt^2} + R_{\mathrm{MS}}\frac{dx}{dt} + K_{\mathrm{MS}}x. \tag{3}$$

Choosing $y_1=x$, $y_2=v$, $y_3=i$, and $y_4=i_2$ as state variables enables us to rewrite Eqs. (1)–(3) into the following state-space equation:

$$\begin{bmatrix} \dot{y}_1 \\ \dot{y}_2 \\ \dot{y}_3 \\ \dot{y}_4 \end{bmatrix} = \begin{bmatrix} 0 & 1 & 0 & 0 \\ \dfrac{-1}{(M_{\mathrm{MS}}+M_{A1})C_{\mathrm{MS}}(x)} & \dfrac{-R_{\mathrm{MS}}}{(M_{\mathrm{MS}}+M_{A1})} & \dfrac{Bl(x)+\frac{1}{2}\frac{dL_E(x)}{dx}y_3}{(M_{\mathrm{MS}}+M_{A1})} & \dfrac{\frac{1}{2}\frac{dL_2(x)}{dx}y_4}{(M_{\mathrm{MS}}+M_{A1})} \\ 0 & \dfrac{-Bl(x)-\frac{dL_E(x)}{dx}y_3}{L_E(x)} & \dfrac{-(R_E(T_V)+R_2(x))}{L_E(x)} & \dfrac{R_2(x)}{L_E(x)} \\ 0 & 0 & \dfrac{R_2(x)}{L_2(x)} & \dfrac{-R_2(x)-\frac{dL_2(x)}{dx}y_2}{L_2(x)} \end{bmatrix} \begin{bmatrix} y_1 \\ y_2 \\ y_3 \\ y_4 \end{bmatrix} + \begin{bmatrix} 0 \\ 0 \\ 1 \\ \dfrac{}{L_E(x)} \\ 0 \end{bmatrix} u. \tag{4}$$

Numerical integration algorithms such as Runge–Kutta method[27] can readily be applied to solve the state-apace equation for the nonlinear responses. Once the velocity $y_2=v$ is obtained, the far field sound pressure can be readily calculated using a baffled point source model

$$p(t,r) = \frac{\rho_0}{2\pi r}S_d\frac{dv}{dt}e^{-j2\pi f_2(r-x)/c}, \tag{5}$$

where r is the distance between the diaphragm and the listening position, ρ_0 is the density of air, and c is the speed of sound.

In the present work, we mainly focus on the nonlinear distortions that generally occur at low frequencies, where the wavelength is large as compared to the speaker dimension and Eq. (5) suffices to model the nonlinear system with acceptable accuracy.

C. Nonlinear measures of symptoms

A single tone is used as a stimulus in harmonic distortion measurements. The nth harmonic distortion associated with the excitation frequency f_1 is defined as

$$\mathrm{HD}_n = \frac{|P(nf_1)|}{P_t}\cdot 100\,\%, \tag{6}$$

where $P(nf_1)$ is the complex spectrum of the sound pressure p at the nth harmonic, and P_t is the rms value of the total signal within an averaging time T

$$P_t = \sqrt{\frac{1}{T}\int_0^T p(t)^2 dt}. \tag{7}$$

In addition, total harmonic distortion (THD) is a common nonlinear measure for a signal with n significant harmonics:

$$\mathrm{THD} = \frac{|P(2f_1)|^2 + |P(3f_1)|^2 + \ldots + |P(nf_1)|^2}{P_t} \times 100\,\%. \tag{8}$$

The dc component of displacement X_{dc} is also a useful measure for evaluating suspension asymmetries.

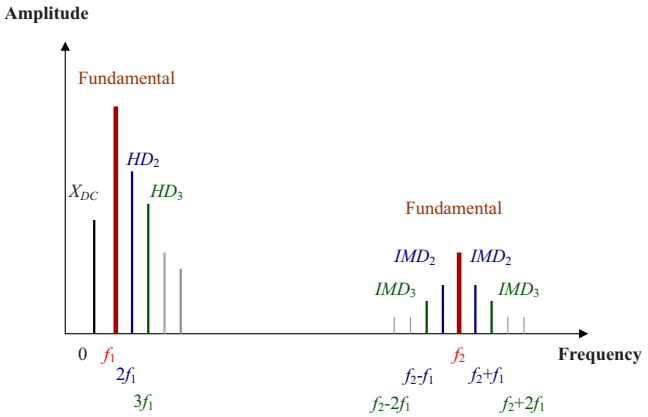

FIG. 2. (Color online) The generic frequency spectrum of a state variable, e.g., sound pressure p, displacement x, and input current i, generated by the two-tone stimulus.

$$X_{\mathrm{dc}} = \frac{|X(0)|}{X_t} \times 100\ \%\ , \tag{9}$$

where $X(0)$ is the dc-component in the complex spectrum of the cone displacement x and X_t is the rms value of the displacement x.

Apart from the preceding single tone measures, a two-tone (f_1 and f_2) stimulation recommended in the IEC standard 60268-5 (Ref. 18) is also utilized for assessing nonlinear loudspeaker symptoms. The excitation signal can be expressed as

$$u(t) = U_1 \sin(2\pi f_1) + U_2 \sin(2\pi f_2). \tag{10}$$

Therefore, an important nonlinear measure is the intermodulation distortion (IMD). IMD accounts for extra frequency components due to intermodulations occurring at $f_2 \pm nf_1$ ($n=1,2,\ldots$), as depicted in Fig. 2. The nth-order IMD associated with f_2 is defined as

$$\mathrm{IMD}_n = \frac{|P(f_2-(n-1)f_1)| + |P(f_2+(n-1)f_1)|}{|P(f_2)|} \times 100\ \%\ . \tag{11}$$

D. Creating a database of loudspeaker causes

A database documenting the relationships between causes and symptoms of loudspeaker nonlinearities is required for training the neural-fuzzy system. Instead of gathering data from real loudspeakers, which is extremely tedious and impractical, we opt for synthetic data obtained using large signal simulations with prescribed nonlinearities.

Among the frequently encountered loudspeaker nonlinearities,[9,10] six common defects are investigated in this paper: (a) asymmetry in $C_{\mathrm{MS}}(x)$, (b) dc-displacement of voice coil offset, (c) asymmetry in $L_E(x)$, (d) coil height (the height of voice coil exceed the air gap), (e) symmetrical limiting of suspension (the rate of change of suspension compliance with respect to cone displacement), and (f) Doppler effect.

Each nonlinear cause leads to unique symptoms of distortions, as summarized in Table II.[9] The entries marked with crosses in Table II indicate that a strong link exists between the nonlinearity and the distortion. The nonlinear causes in a loudspeaker's response can be subdivided into three categories, "critical nonlinearity variation," "asymmetric nonlinearity," and "Doppler effect," as follows:

1. Critical nonlinearity variation: "Coil height" and "symmetrical limiting of suspension"

Large cone excursion in general forces the voice coil to leave the air gap and the suspension to be overstretched. This gives rise to nonconstant symmetric $C_{\mathrm{MS}}(x)$ and $Bl(x)$ curves.[9,10] A symmetric curve usually produces the third- and other odd-order distortion components. To simulate the coil height and the "suspension limiting" defect, the second-degree term of the Bl and the C_{MS} series are usually multiplied by a factor $\beta > 1$ to increase variations, where x denotes the displacement of voice coil from the rest position.

$$Bl'(x) = b_0 + b_1 x + \beta b_2 x^2 + \sum_{i=3}^{n} b_i x^i, \tag{12}$$

$$C'_{\mathrm{MS}}(x) = c_0 + c_1 x + \beta c_2 x^2 + \sum_{i=3}^{n} c_i x^i. \tag{13}$$

2. Asymmetric nonlinearity: "Coil offset" and "asymmetry in $C_{\mathrm{MS}}(x)$ and $L_E(x)$"

Asymmetric nonlinearities generally result in the second- and other even-order distortion components. Asymmetric $Bl(x)$ and $C_{\mathrm{MS}}(x)$ curves can arise due to imperfection in loudspeaker manufacturing. These defects can be modeled by shifting the $Bl(x)$ and $C_{\mathrm{MS}}(x)$ curves by a small constant ε.

TABLE II. Relationship between nonlinear causes and symptoms of moving-coil loudspeakers.

Physical cause	X_{dc}	HD_2	HD_3	IMD_2	IMD_3	$IMD_{l,i}$
Coil offset		X		X		
Coil height			X		X	
Asymmetry in $C_{\mathrm{MS}}(x)$	X	X				
Symmetrical limiting of suspension			X			
Asymmetry in $L_E(x)$				X		X
Doppler effect				X		

$$Bl'(x) = Bl(x-\varepsilon) = \sum_{i=0}^{n} b_i (x-\varepsilon)^i, \tag{14}$$

$$C'_{\mathrm{MS}}(x) = C_{\mathrm{MS}}(x-\varepsilon) = \sum_{i=0}^{n} c_i (x-\varepsilon)^i. \tag{15}$$

The inductance $L_E(x)$ without shorting ring also has an asymmetric curve. To model this, we multiply the linear term of the L_E series by a factor $\beta > 1$ to yield

$$L'_E(x) = l_0 + \beta l_1 x + \sum_{i=2}^{n} l_i x^i. \tag{16}$$

3. Doppler effect

Doppler distortion generally arises because of large cone displacement in low frequencies at which the loudspeaker behaves as a moving source. The low frequency displacement is so large that the high frequency signal riding on the top of this low frequency signal is effectively changing its position. This is not very critical for low frequency component itself but causes intermodulation of high frequency signals with a short wavelength. This effect leads to frequency shift, which in turn increases IMD by 6 dB/octave toward higher frequencies.[9,13] This effect can be simulated by increasing the frequency of the second tone f_2 in Eq. (5). That is,

$$p(t,r) = \frac{\rho_0}{2\pi r} S_d \frac{dv}{dt} e^{-j2\pi(f_2+\Delta f_2)(r-x)/c}, \tag{17}$$

where Δf_2 denotes the frequency shift of f_2. The Doppler distortion arises because the second frequency is also present and its distance (between source and listener) is modulated. The cone excursion could be only a few centimeters. However, this distance between the source and the listener varies enough to give rise to Doppler effect. It is as if the high frequency source is moving back and forth, thus giving rise to the shifting in pitch.

In order to establish a database that incorporates all the aforementioned loudspeaker nonlinearities, a hybrid approach is undertaken. We begin with identifying the parameters of three real loudspeakers and then carrying out numerical simulations by varying β and ε in Eqs. (12)–(16) and input voltage to produce synthetic data. A total of 700 sets of nonlinear causes and symptoms are created for the database using this approach.

III. INFERRING NONLINEAR DEFECTS USING NEURAL-FUZZY SYSTEMS

In this paper, the FNN (Ref. 21) is utilized for the loudspeaker diagnostic problem. The six nonlinear causes and their associated symptoms summarized in Table II are selected for the input and output layers of the FNN, respectively. The FNN with a fuzzy rule-based model embedded in a NN carries out intelligent inference with combined advantages of both artificial NN and fuzzy logic. On the basis of the preceding database, the FNN is trained to deal with unknown nonlinear diagnostic problems of loudspeakers. Figure 3 illustrates the five layers in the FNN: the input layer, the input membership layer, the fuzzy rule layer, the output membership layer, and the conclusion layer. The function of each layer is explained next.

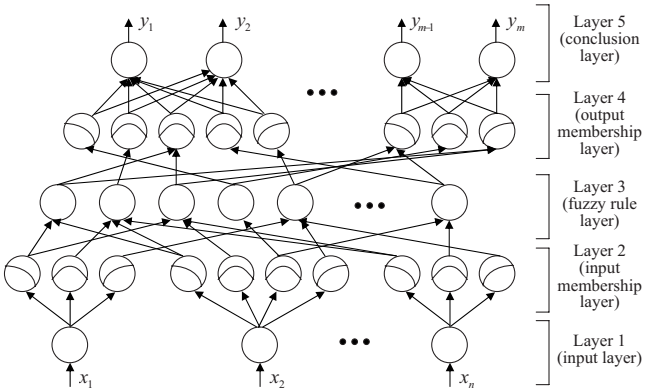

FIG. 3. The schematic of a McCulloch–Pitts neuron.

Unlike classical sets representing only binary states, *true* or *false*, the fuzzy sets use a membership function to determine the degree of "truth." Let $\tilde{A}$ be a fuzzy set and U be its *universe of discourse*

$$\tilde{A} = \{(x, \mu_{\tilde{A}}(x)) | x \in U\}, \tag{18}$$

where $\mu_{\tilde{A}}(x)$ is the membership function that represents the degree of x belonging to the fuzzy set $\tilde{A}$, and its value is always within the interval [0,1]. In this FNN, the input membership layer consists of several membership functions, "minor," "moderate," and "Severe," to indicate various levels of nonlinear distortions. The output membership layer consists of two membership functions representing "having this problem" and "not having this problem," respectively. The output membership function returns the probability ranging from 0% to 100% for each nonlinear cause. The core of the FNN is the fuzzy rule layer that associates the input membership layer and the output membership layer to realize the following "if-then" rule:

$$\text{Rule } i\text{: if } (x_1 \text{ is } A_{i1} \text{ and} \cdots \text{and } x_n \text{ is } A_{in})$$

$$\text{then } (y_1 \text{ is } B_{i1} \text{ and} \cdots \text{and } y_n \text{ is } B_{in}), \tag{19}$$

where A_{ij} and B_{ij} are the input and output fuzzy sets, respectively. Finally, the conclusion layer serves as a *defuzzifier* and makes an inference of fault type by using the mean of centric method.[21]

Figure 4 illustrates one basic element of the FNN, usually called an *M-P neuron*. This jth processing element computes a weighted sum of its inputs and then exports the output o_j:

$$o_j(t+1) = f\left(\sum w_{ij} x_i(t)\right), \tag{20}$$

where f is a threshold function such as the *sigmoid function*[22] in which the relationship between the input x and the output $f(x)$ is given by

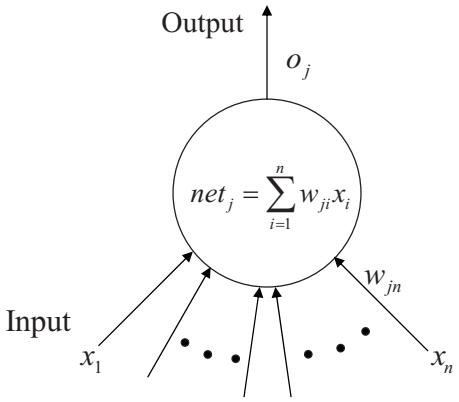

FIG. 4. The structure of the FNN, where $x's$ and $y's$ denote the input and output variables, respectively.

$$f(x) = \frac{1}{1 + e^{-x}}. \tag{21}$$

The neurons in the five layers of the FNN are interconnected by synapses.

At the initial stage, each synaptic weight in the FNN is set to be a random number. No rules exist between the input and output membership layers. The membership functions in the input and output membership layers are initially set by experience, as shown in Figs. 5(a) and 5(b). Next, at the training stage, a learning process is carried out to create

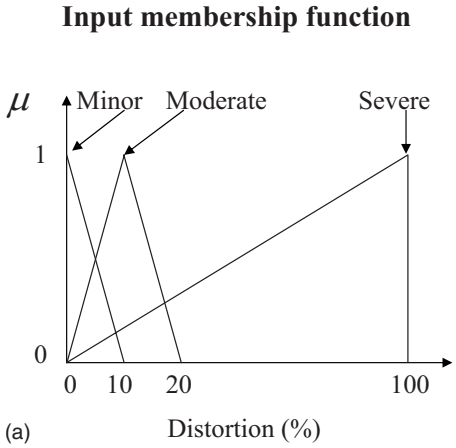

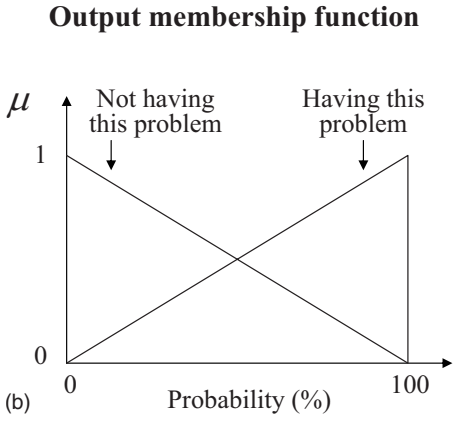

FIG. 5. The membership functions and the linguistic terms in the fuzzy logic system. (a) The input membership function. (b) The output membership function.

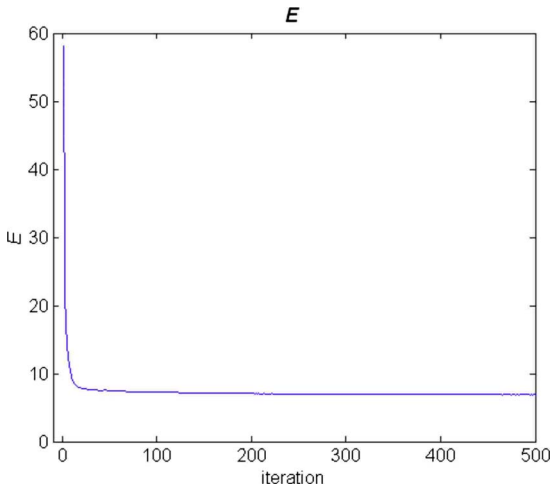

FIG. 6. (Color online) The membership functions of rule 1 and rule 2 in the fuzzy rule layer.

fuzzy rules and adjust the neural weights and the membership functions by using the preceding database. An error function E is defined for the network learning

$$E = \frac{1}{2} \sum_i (y_i - y_i')^2, \tag{22}$$

where y_i is the ith expected output and y' is the ith calculated output. A supervised learning algorithm with backpropagation[22] is employed to minimize the error function. In the algorithm, the increment of the weight w_{ij}^n at time t is updated according to

$$\Delta w_{ij}^n(t) = \eta \times \frac{\partial E}{\partial w_{ij}^n} + \alpha \times \Delta w_{ij}^n(t-1), \tag{23}$$

where $\Delta w_{ij}^n(t)$ is the increment of the weight between the ith neuron of the $(n+1)$th layer and the jth neuron of the nth layer at time t, η is the learning factor, and α is the momentum term for accelerating the convergence. As soon as the error decreases to an acceptable range, the training is terminated. To be specific, 500 and 200 cases out of the preceding database are used for training and verification, respectively. Figure 6 shows the learning curve of this FNN, where the system error reduces from 58 to 6.9 after 500 iterations. A judicious choice of 70% threshold indicates whether or not a loudspeaker under test has a particular nonlinear cause. To verify the FNN, in-group tests of the remaining 200 cases were conducted, with results summarized in Table III. A very successful detection rate was achieved using the network (average rate of correct inference=97.0%).[28,29]

An example for the FNN system is given as follows. Assume that two rules exist in training fuzzy network.

(1) If HD3 is moderate and IMD3 is minor, then it may have "coil height" problem.
(2) If HD3 is moderate and IMD3 is moderate, then it may not have coil height problem.

Two weighting factors W_1 and W_2 are given to those two rules in the FNN system. The membership functions of HD3 and IMD3 obtained after training are shown Fig. 7. For in-

TABLE III. Results of the in-group test of the FNN diagnostic system.

Nonlinear cause	Number of case	Rate of correct inference	Rate of incorrect inference
Normal	36	100%	0%
Asymmetry in $C_{MS}(x)$	14	100%	0%
Coil offset	13	100%	0%
Asymmetry in $L_E(x)$	12	100%	0%
Coil height	13	100%	0%
Symmetrical limiting of suspension	19	100%	0%
Doppler effect	14	100%	0%
Asymmetry in $C_{MS}(x)$+ coil offset	26	88.4%	11.6%
Asymmetry in $C_{MS}(x)$+ Asymmetry in $L_E(x)$	12	100%	0%
Asymmetry in $L_E(x)$+ coil offset	23	95.7%	4.3%
Symmetrical limiting of suspension+coil height	18	88.9%	11.1%
Total number of cases=200			
Average rate of correct inference=97.0%			

stance, the distortion data HD3=10% and IMD3=15% correspond to 0.5 minor and 0.5 moderate in HD3. The same data correspond to 0.25 minor and 0.75 moderate in IMD3. Next, calculate the "degree of detonation" for each rule:

$$\text{Rule } 1 = W_1 \times 0.5 \times 0.25, \tag{24}$$

$$\text{Rule } 2 = W_2 \times 0.5 \times 0.75. \tag{25}$$

Then, according to the degree of detonation, inference of the defect coil height can be drawn, or "defuzzified," using the certainty equivalent principle.[22]

IV. EXPERIMENTAL INVESTIGATIONS

Figure 8 illustrates the architecture of the expert diagnostic system proposed in this paper. Two loudspeakers denoted as Drivers A and B were employed in the case study to examine the diagnostic performance of this expert diagnostic system. The parameters of these two loudspeakers are summarized in Table IV. Figure 9 shows the experimental ar-

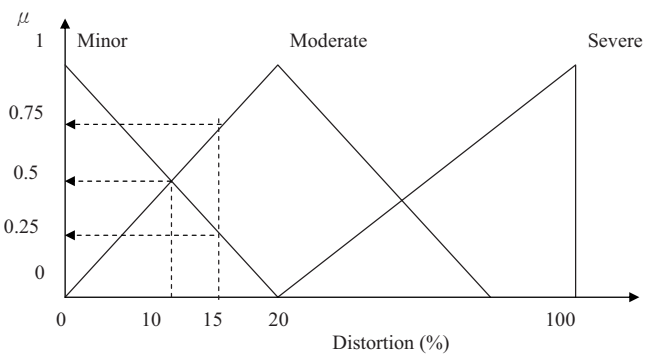

FIG. 7. The learning curve (error vs iteration) obtained in the training phase of the FNN system.

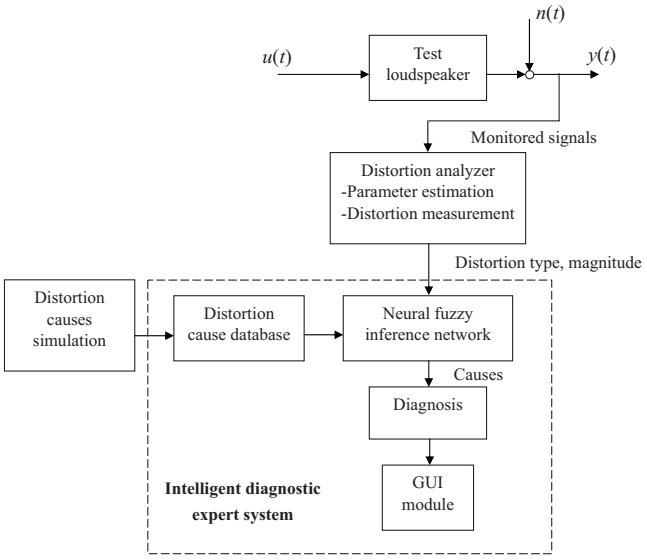

FIG. 8. The block diagram of the expert diagnostic system. The intelligent diagnostic system comprises a defect database and an inference engine marked by the dotted line.

arrangement inside an anechoic room, where the test conditions follow the IEC 60268-5, i.e., $U_1=4U_2$, $f_1=f_S$, $f_2=8.5f_1$. The bass tone voltage U_1 was chosen according to the rated power of the loudspeaker. A laser vibrometer and a microphone were used to measure cone displacement and sound pressure, respectively.

Nonlinear measurements obtained by the Klippel Distortion Analyzer 2 (Rev. 2.0)6 (Refs. 6 and 30) are summarized in Table V. Hence, the proposed FNN diagnostic system was applied to infer the nonlinear defects of the loudspeaker under test. The results are summarized in Table VI. To further explore the inference capability of the proposed FNN loudspeaker diagnostic system, a numerical simulation is undertaken. Although the finite element modeling is an alternative approach,[31] it is simply too time consuming to produce sufficient number of sample data. For the present multidomain

TABLE IV. Thermal and nonlinear parameters at the rest position.

Parameter	Driver A	Driver B	Unit
f_S	60	140	Hz
C_{MS} $(x=0)$	1.22	4.21	mm/N
Bl $(x=0)$	8.51	2.81	N/A
L_E $(x=0)$	1.20	0.25	mH
L_2 $(x=0)$	1.41	0.49	mH
M_{MS}	13.19	1.78	gm
Q_{MS}	1.91	4.21	
R_E	7.24	9.04	Ω
R_2 $(x=0)$	5.64	1.05	Ω
R_{TV}	14.05	14.96	K/W
R_{TM}	30.75	9.44	K/W
C_{TV}	2.56	0.97	J/K
C_{TM}	68.56	74.96	J/K
Normal rated power	5	3	W
S_D	78.54	28.27	cm^2

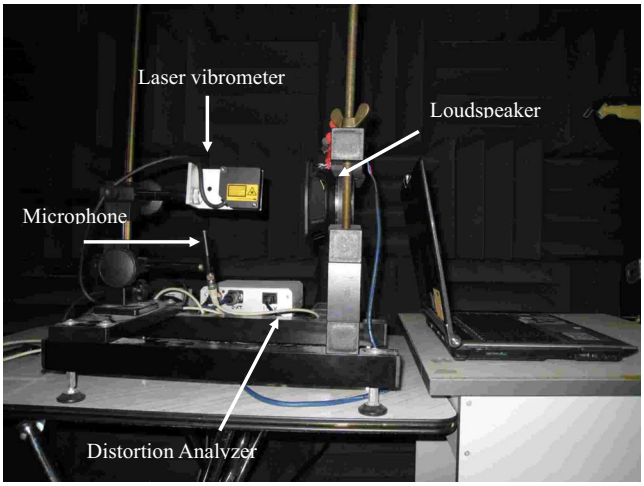

FIG. 9. (Color online) The experimental arrangement of the FNN loudspeaker diagnostic system.

problem that involves the electrical, mechanical, and acoustical subsystems, coupling these different physical domains results in a complicated set of matrix equations that are not trivial to solve simultaneously. We thus opt for more efficient analogous circuit approach in this paper. In the simulation, only one kind of nonlinearity is taken into account at a time, while keeping the remaining parameters the same as the rest position. By doing so, it is easier to validate the inference result and to assess the sensitivity of each nonlinear parameter.

A. Loudspeaker A

Driver A is a 10 cm diameter woofer with a resonance frequency of 60 Hz. Figure 10 shows the frequency response of the diaphragm displacement under the condition $U_1=6V$, where the displacement at 40 Hz is about 3 mm. The large signal parameters $Bl(x)$ and $C_{\mathrm{MS}}(x)$ measured by the distortion analyzer are shown in Figs. 11(a) and 11(b). In contrast to the nearly constant characteristics of $Bl(x)$ and $C_{\mathrm{MS}}(x)$, the voice coil inductance $L_E(x)$ shown in Fig. 11(c) has a distinct asymmetrical shape increasing toward the negative displacement.

Measured data in Table V reveals that Driver A suffers from high second-order intermodulation both in sound pressure and current. For this loudspeaker, the proposed FNN system inferred that an asymmetric $L_E(x)$ problem could exist with probability nearly 100% (Table VI). To validate this result, nonlinear simulations were conducted next.

In Fig. 12(a), the nonlinear simulation reveals that harmonic distortions are almost negligible ($<7\%$ above 50 Hz). On the other hand, a two-tone signal comprising a tone fixed at the frequency $f_1=60$ Hz and a tone with varying frequency f_2 is employed to excite intermodulations, as shown in Fig. 12(b). The third-order intermodulation components in sound pressure and current of Driver A are both very small ($<8\%$) in the wide frequency range. However, very high second-order intermodulations ($>20\%$) is clearly visible in Fig. 12(b). The fact that the intermodulation in current is comparable with that in sound pressure or the IMD increases at high frequencies suggests that the primary cause of nonlinearity could be asymmetry in $L_E(x)$.

Figure 12(c) shows a simulation result for the second-order intermodulation. Obviously, the asymmetry of the $L_E(x)$ (represented as a solid line marked with asterisks) is the dominant source of the second-order IMD because this curve reaches a level close to the response when all nonlinearities are involved.

In summary, the preceding analysis reveals that asymmetry in $L_E(x)$ is the dominant nonlinear cause, which agrees very well with the result inferred by the FNN system. A remedy to such problem is to place conductive materials such as conducting rings or caps made of aluminum or copper on the pole piece of the loudspeaker.[18]

B. Loudspeaker B

The driver B is a 6 cm woofer with a deviating voice coil. Figure 13 shows the frequency response of the diaphragm displacement under the condition $U_1=5$ V, where the maximum displacement is about 1.4 mm at 140 Hz. The $Bl(x)$ curve shown in Fig. 14(a) implies a distinct asymmetry, for the force factor decreases much faster at negative displacement than at positive displacement. Also, the compliance $C_{\mathrm{MS}}(x)$ shown in Fig. 14(b) is limited at the negative displacement because the variation of the compliance at $x=-1.5$ mm reduces to almost 55% of the maximum value. Comparing with the inductance of driver A reveals that the inductance of driver B is not that high but also has an asymmetrical characteristic, as shown in Fig. 14(c). Table V reveals that driver B suffers from high third-order harmonic distortion and the second- and third-order intermodulations. With FNN inference, high probabilities associated with coil offset, coil height, and symmetrical limiting of suspension summarized in Table VI indicate that there could be design flaws in the suspension and voice coil of driver B. To validate this result, nonlinear simulations were conducted next.

TABLE V. Distortion measures. Boldface indicates a significant distortion.

	X_{DC}	HD_2	HD_3	IMD_2	IMD_3	$\mathrm{IMD}_{2,i}$
Driver A	7.6%	3.8%	0.7%	**13.1%**	6.2%	**18.8%**
Driver B	8.5%	4.1%	**20.2%**	**26.0%**	**11.2%**	0.8%

The harmonic distortions measured at input voltage $U_1 = 5$ V are shown in Fig. 15(a). Clearly, the second-order harmonic distortion is not significant, whereas the third-order harmonic distortion exceeding 20% below the resonance frequency could degrade sound quality at low frequencies. Figure 15(a) shows a simulation result for the third-order harmonic distortion. At low frequencies, comparison between the measured result, the prediction considering all nonlinearities, and the prediction considering only nonlinearity of $C_{MS}(x)$ reveals that large third-order harmonic distortion is predominantly caused by symmetrical limiting of suspension. Above 200 Hz, disagreement between prediction and the measurement starts to show because the lumped parameter model fails to model the flexural modes of the diaphragm at high frequencies.

A two-tone stimulus with $f_1 = 140$ Hz, $f_2 = 900-3000$ Hz, $U_1 = 5$ V, $U_2 = U_1/4$ is utilized for measuring the intermodulations. In Fig. 15(b), the measured second-intermodulation and the third-intermodulation well exceed the 10% threshold. Figure 16(b) shows a simulation result for the third-order intermodulation. The measured data (dashed line) are nearly constant (10%) independent of the varying frequency f_2, which is a unique feature of intermodulations resulting from $Bl(x)$ nonlinearity. After switching off all nonlinearities and considering only the force factor $Bl(x)$, we obtain a prediction almost identical to the measurement. Thus, it can be concluded that the symmetric $Bl(x)$ nonlinearity is the primary source of the third-order IMD.

The simulation results of the second-order intermodulation are presented in Fig. 16(c). Again, the $Bl(x)$ nonlinearity contributes significantly to the second-order intermodulation by its critical asymmetry. Although the distortions due to nonlinear $L_E(x)$ and Doppler effect rise by 6 dB/octave, their importance is not as high as that of $Bl(x)$ nonlinearity below 3000 Hz.

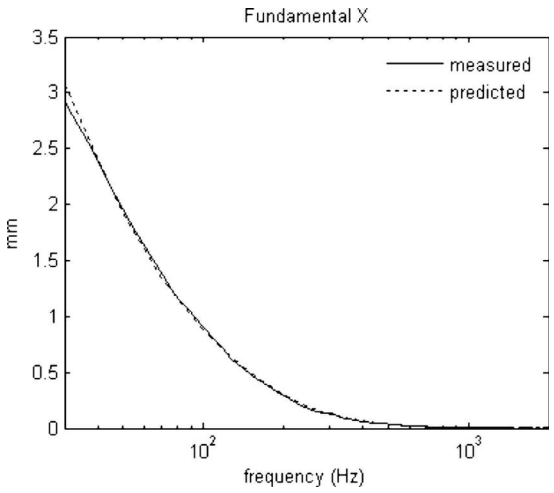

FIG. 10. Fundamental displacement x of driver A predicted (dotted line) and measured (solid line) at an input voltage of 6 V.

In summary, the diagnostic results of numerical simulation agree well with the results inferred by the FNN system. It can also be seen from this result that the FNN system is capable of dealing with not only single-cause but also multiple-cause problems.

V. CONCLUSIONS

A neural-fuzzy-based expert system has been developed for moving-coil loudspeaker diagnostics. The system was established in two stages. First, a cause-symptom database of loudspeaker nonlinearity was created on the basis of a large signal model. Second, the nonlinear causes and symptoms in the database were used as the input and output in training the neural-fuzzy system. A number of distortion indices were measured for the loudspeaker under test using a distortion analyzer. With the distortion indices as the input, the fault types of the loudspeaker can be determined using the FNN system, much like a human expert.

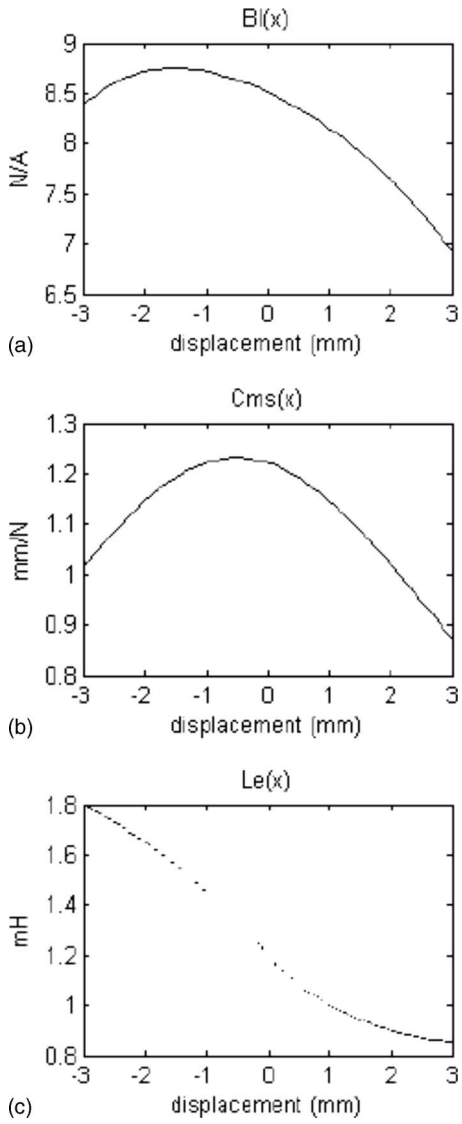

FIG. 11. Nonlinearities of driver A plotted versus displacement x. (a) Force factor $Bl(x)$. (b) Compliance $C_{MS}(x)$. (c) Inductance $L_E(x)$.

TABLE VI. Probability of defect inferred by the FNN diagnostic system. Boldface indicates a highly possible cause of nonlinearity.

	Coil offset	Coil height	Asymmetry in $C_{MS}(x)$	Suspension limiting	Asymmetry in $L_E(x)$	Doppler effect
Driver A	2%	0%	0%	0%	**99%**	2%
Driver B	**98%**	**100%**	26%	**98%**	0%	2%

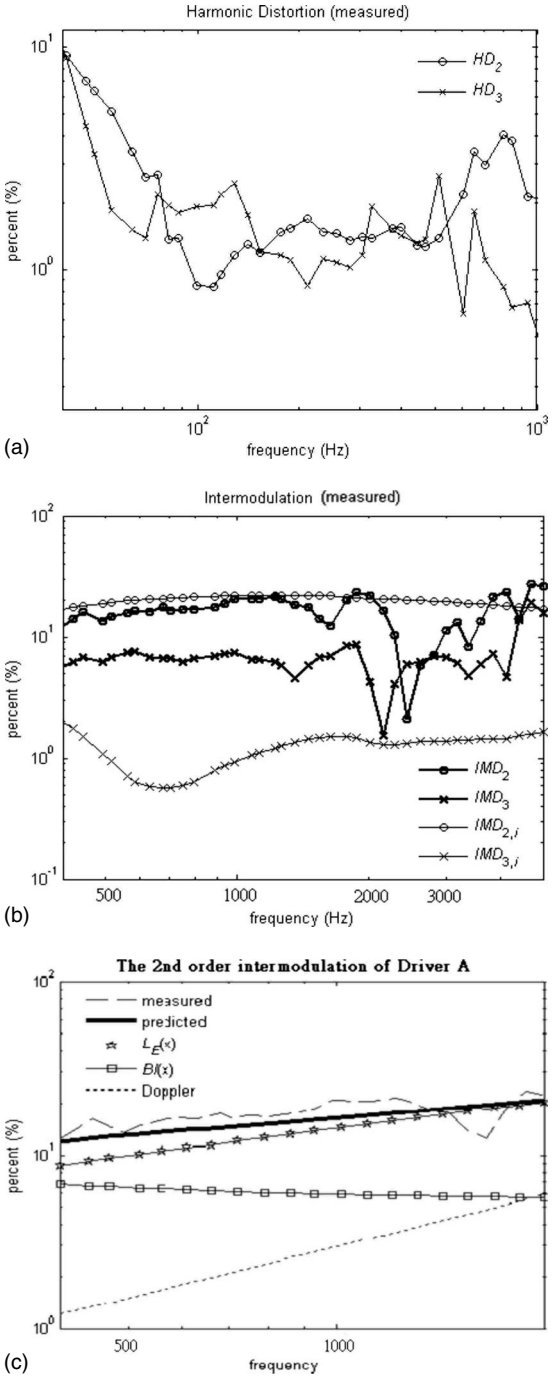

FIG. 12. The nonlinear distortions of driver A measured using the distortion analyzer. (a) The second- and third-order harmonic distortions. (b) The second- and third-order intermodulations. (c) The second-order intermodulations of driver A: measured data (dashed line), predicted data with all nonlinearities considered (solid line), and separate nonlinearities.

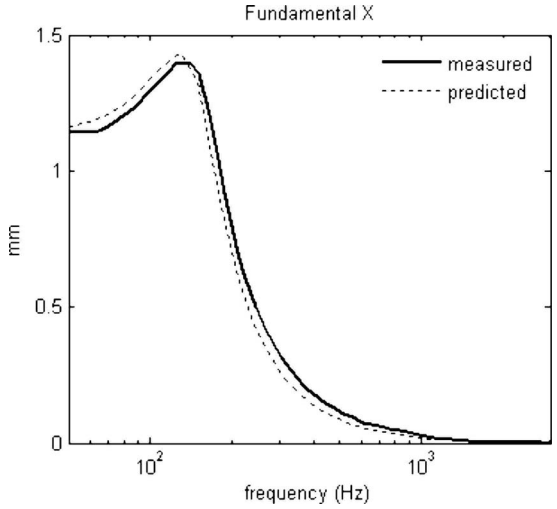

FIG. 13. Fundamental displacement x of driver B predicted (dotted line) and measured (solid line) at an input voltage of 5 V.

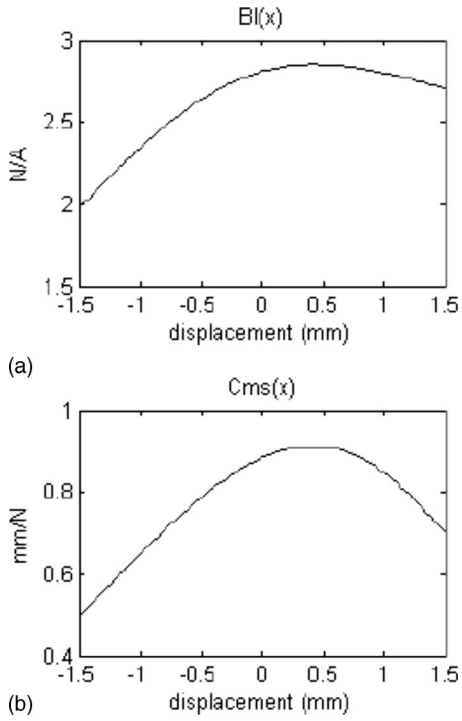

FIG. 14. Nonlinearities of driver B plotted vs displacement x. (a) Force factor $Bl(x)$. (b) Compliance $C_{MS}(x)$. (c) Inductance $L_E(x)$.

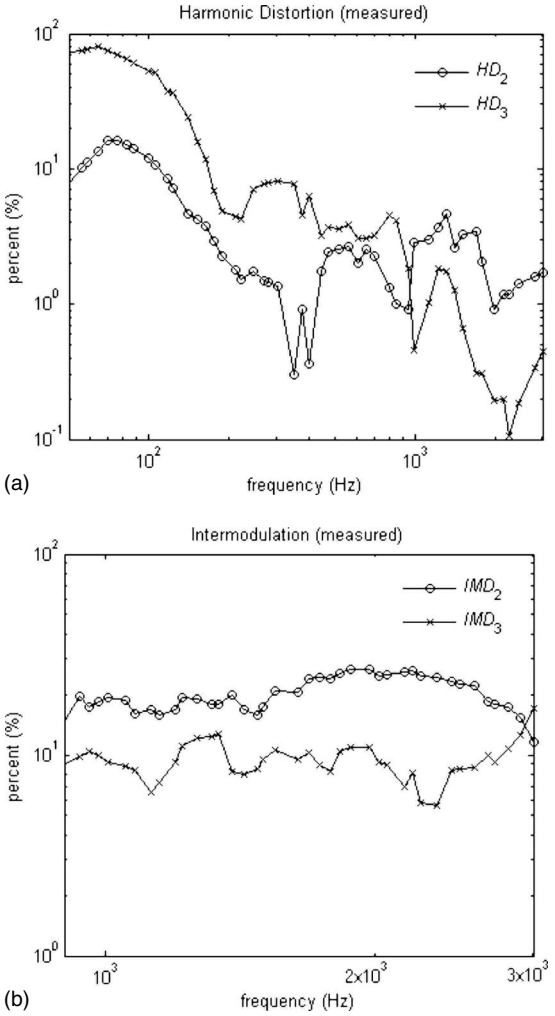

FIG. 15. The nonlinear distortions of driver B measured by the distortion analyzer. (a) The second- and third-order harmonic distortions. (b) The second- and third-order intermodulations.

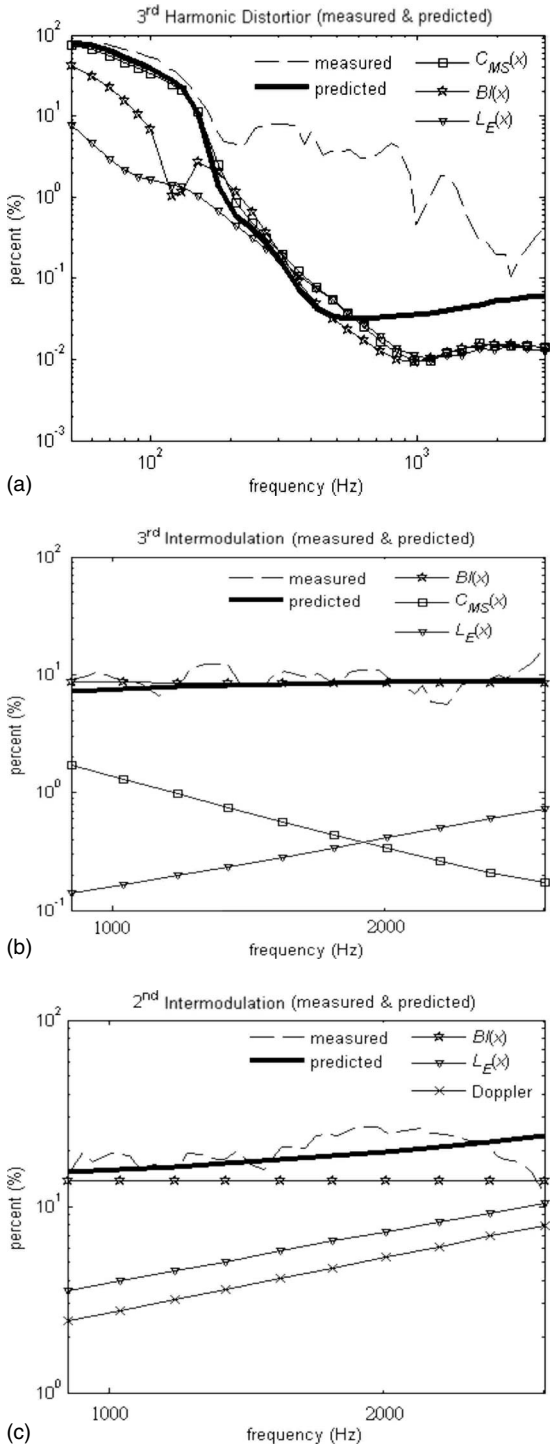

FIG. 16. Distortions of driver B measured (dashed line), predicted with all nonlinearities considered (solid line) and separate nonlinearities. (a) The third-order harmonic distortions. (b) The third-order intermodulations. (c) The second-order intermodulations.

This neural-fuzzy diagnostic system has been justified by experiments for two sample loudspeakers. The results inferred by the FNN diagnostic system was in good agreement with those obtained using numerical prediction. The results revealed that the proposed diagnostic system was capable of identifying single cause but also multiple causes of loudspeakers. This FNN system provides a more accurate and cost-effective solution of loudspeaker diagnostics than human experts. However, the present system is more cost effective than human experts and is only true if the diagnostics performed by a human expert is based on distortion measurements. However, the proposed methodology could still be of some value since systems for measuring the nonlinear loudspeaker parameters such as $B_l(x)$ and $C_{\mathrm{MS}}(x)$ are not widely available, as compared to distortion analyzers.

Several extensions of the present work are under way. The system is being converted to a fully on-line test bench, as required in quality control of mass production. The diagnostic capability of the system shall be enhanced by incorporating more fault types such as the rub and buzz problem and thermal buildup problem, etc., into the present system.

ACKNOWLEDGMENT

The work was supported by the National Science Council in Taiwan, Republic of China, under the Project No. NSC91-2212-E009-032.

[1]J. Borwick, *Loudspeaker and Headphone Handbook* (Focal, Oxford, UK, 1994).
[2]B. Elliott, "On the measurement of the low-frequency parameters of moving-coil piston transducers," 58th Convention of the Audio Engineer-

ing Society, New York, November, 1977.
[3]M. H. Knudsen, "Low-frequency loudspeaker models that include suspension creep," J. Audio Eng. Soc. **41**, 3–18 (1993).
[4]R. H. Small, "Direct-radiator loudspeaker system analysis," J. Audio Eng. Soc. **20**, 383–395 (1972).
[5]W. Klippel, "Nonlinear large-signal behavior of electrodynamic loudspeakers at low frequencies," J. Audio Eng. Soc. **40**, 483–496 (1992).
[6]W. Klippel, "Distortion analyzer—A new tool for assessing and improving electrodynamic transducer," presented at the 108th Convention of the Audio Engineering Society, Paris, 19–22 February, 2000.
[7]H. Huang, "Analysis of nonlinear behavior of loudspeakers using the instantaneous frequency," J. Acoust. Soc. Am. **113**, 2202 (2003).
[8]W. Klippel, "Measurement of loudspeaker parameters by inverse nonlinear control," J. Acoust. Soc. Am. **105**, 1359 (1999).
[9]W. Klippel, "Loudspeaker nonlinearities—Causes, parameters, symptoms," presented at 119th Convention of the Audio Engineering Society, New York, 7–10 October, 2005.
[10]W. Klippel, "Assessment of voice-coil peak displacement Xmax," J. Audio Eng. Soc. **51**, 307–324 (2003).
[11]D. Clark, "Precision measurement of loudspeaker parameters," J. Audio Eng. Soc. **45**, 129–141 (1997).
[12]J. D'Appolito, *Testing Loudspeakers* (Audio Amateur, New York, 1998).
[13]W. Klippel, "Prediction of speaker performance at high amplitudes," presented at the 111th Convention of the Audio Engineering Society, New York, 21–24 September, 2001.
[14]A. J. M. Kaizer, "Modeling of the nonlinear response of an electrodynamic loudspeaker by a Volterra series expansion," J. Audio Eng. Soc. **35**, 421–433 (1987).
[15]W. Klippel, "Nonlinear modeling of the heat transfer in loudspeakers," J. Audio Eng. Soc. **52**, 3–25 (2004).
[16]W. Klippel, "Dynamic measurement and interpretation of the nonlinear parameters of electrodynamic loudspeakers" J. Audio Eng. Soc. **38**, 944–955 (1990).
[17]E. R. Olsen and K. B. Christensen, "Nonlinear modeling of low frequency loudspeakers—A more complete model," The 100th Convention Audio Engineering Society, Copenhagen, 11–14 May, 1966.
[18]W. Klippel, "Diagnosis and remedy of nonlinearities in electrodynamical transducers," presented at the 109th Convention of the Audio Engineering Society, Los Angeles, 21–25 September, 2000.
[19]P. Jackson, *Introduction to Expert Systems* (Addison-Wesley, Reading, MA, 1986).
[20]L. A. Zadeh, "Fuzzy sets as a basis for a theory of possibility," Fuzzy Sets Syst. **1**, 3–28 (1978).
[21]T. Kohonen, "An introduction to neural computing," Neural Networks **1**, 3–16 (1988).
[22]C. T. Lin and C. S. George Lee, *Neural Fuzzy Systems* (Prentice-Hall, Englewood Cliffs, NJ, 1966).
[23]M. Becraft and R. Isermann, "Neuro-fuzzy systems for diagnosis," Fuzzy Sets Syst. **89**, 289–307 (1997).
[24]M. R. Bai, I. L. Hsiao, H. H. Tsai, and C. T. Lin, "Development of an on-line diagnosis system for rotor vibration via model-based intelligent inference," J. Acoust. Soc. Am. **107**, 315–323 (2000).
[27]C. F. Juang and C. T. Lin, "An on-line self-constructing neural fuzzy inference network and its applications," IEEE Trans. Fuzzy Syst. **6**, 12–13 (1998).
[28]J. H. Mathews and K. K. Fink, *Numerical Methods Using Matlab* (Prentice-Hall, Upper Saddle River, NJ, 1966).
[25]W. Klippel, "Measurement of impulsive distortion, rub and buzz and other disturbances," Klippel GmbH, www.klippel.de (Last viewed June 2008).
[26]S. Temme, "Are you shipping defective loudspeakers to your customers?," http://www.listeninc.com/site/notes.html (Last viewed September 2008).
[29]"Sound system equipment. Part 5: Loudspeakers," IEC Publication No. 60268-5.
[30]Specification of the Klippel Analyzer System, Klippel GmbH, www.klippel.de (Last viewed June 2008).
[31]M. Rausch, "Optimization of electrodynamic loudspeaker-design parameters by using a numerical calculation scheme," Acust. Acta Acust. **85**, 412–419 (1999).